DOI 10.5012/bkcs.2011.32.5.1483

Protection Effect of ZrO_2 Coating Layer on $LiCoO_2$ Thin Film

Hye Jin Lee, Sang Cheol Nam,† and Yong Joon Park*

Department of Advanced Materials Engineering, Kyonggi University, Gyeonggi-do 443-760, Korea
**E-mail: yjpark2006@kyonggi.ac.kr*
†GS NanoTech Co., Ltd. 453-2 Seongnae-dong, Gangdong-gu, Seoul 134-848, Korea
Received December 15, 2010, Accepted March 3, 2011

The protection effect of a ZrO_2 coating layer on a $LiCoO_2$ thin film was characterized. A wide and smooth $LiCoO_2$ thin film offers sufficient opportunity for careful observation of the reaction at the interface between cathode (coated and uncoated) and electrolyte. The formation of a ZrO_2 coating on a $LiCoO_2$ thin film was confirmed by secondary ion mass spectrometry. Scanning electron and atomic force microscopy were used to characterize the surface morphologies of coated and uncoated films before and after cycling. A ZrO_2-coated $LiCoO_2$ film showed a higher discharge capacity and rate capability than an uncoated film. This may be associated with a surface protection effect of the coating. The surface of a pristine film was damaged during cycling, whereas the coated film maintained a relatively clear surface under the same measurement conditions. This result clearly demonstrates the protection effect of a ZrO_2 coating on a $LiCoO_2$ thin film.

Key Words : Cathode, ZrO_2, Surface coating, Lithium battery, Thin film

Introduction

Since Sony first announced commercial availability in 1991, lithium ion batteries have served as essential power sources for cellular phones, personal digital assistants (PDAs), laptop computers, and electric vehicles. Among the several components of a lithium ion battery, the cathode, most of all, determines the capacity, cyclic performance, and thermal stability. Therefore, numerous studies have been performed to enhance the properties of cathode materials. One approach to improve the electrochemical properties of a cathode is surface modification by coating with oxides,[1-5] phosphates,[6-10] or fluorides.[11-15] Such surface coating enhances the capacity retention, rate capability and, in some cases, thermal stability, without sacrificing the specific capacity of the cathode. However, the coating effect for cathodes is highly attributable to the specific coating material, coating morphology, and coating content or thickness.[16-19] Thus, a careful characterization of the interface between a coating material and pristine cathode is a key factor to obtain a highly improved cathode material *via* surface coating. However, it has been difficult to characterize this interface reaction because of the small particle size of the pristine powder, very low thickness of the coating layer, and rough surface of the positive electrode. Herein, we introduce a thin film electrode as a pristine cathode to investigate the interface reaction for an electrolyte/coating layer/pristine cathode in detail. The surface of a thin film cathode is much wider and smoother than that of a bulk-type electrode, which may offer sufficient opportunity for careful observation of the interface reaction of a coating layer. In this work, we prepared a ZrO_2-coated $LiCoO_2$ thin film and investigated its electrochemical properties and surface-morphological change during cycling. ZrO_2 is a good coating material for the cathode of lithium ion batteries[1] and $LiCoO_2$ is a commercial cathode material. Therefore, a ZrO_2-coated $LiCoO_2$ thin film could be considered a representative sample for careful characterization of the coating effect of a cathode material.

Experimental

The pristine $LiCoO_2$ thin film was supplied by the GS NanoTech Co. To prepare the ZrO_2 coating solution, zirconium (IV) butoxide $[Zr[O(CH_2)_3CH_3]_4]$ (80 wt % Aldrich) was dissolved in 20 mL of a mixed solvent consisting of distilled water, 1-butanol, and acetic acid. Then, the solution was stirred continuously for 1 h at 25 °C, after which the solution was coated onto the $LiCoO_2$ thin film substrate using a spin-coater (K-359 model S-1, supplied by Kyowariken). The coated $LiCoO_2$ thin films were heat-treated in a rapid thermal annealing (RTA) system at 400 °C for 30 min. The microstructure of the film was observed by field-emission scanning electron microscopy (FE-SEM, JEOL-JSM 6500F) and atomic force microscopy (AFM).

The electrochemical characterization of the coated $LiCoO_2$ films was performed in the non-aqueous half-cells of a three-electrode system at ambient temperature. The active area of each film used for the electrochemical test was about 1 cm × 1 cm. Two Li foil electrodes were used as the counter and reference electrodes. The electrolyte was 1 M $LiClO_4$ in PC. The cells were subjected to galvanostatic cycling using a WonAtech system at constant current densities of 0.2, 0.4, and 0.6 $mA \cdot cm^{-2}$, in a voltage range of 4.25-3.0 V. Secondary ion mass spectrometry (SIMS) analysis was applied for the characterization of the coated and pristine films to obtain information about the constituent elements. The CAMECA IMS-6f Magnetic Sector SIMS at the Korea Basic Science Institute (Busan center) was used for the measurement. A

primary ion beam of Cs+ was used, with a beam energy of 5.0 kV. The beam current was 30 nA, and the raster size was 200 μm × 200 μm.

Results and Discussion

It has been speculated that an important factor in determining the coating effect is the thickness of the coating layer. In this work, the coating thickness was controlled by the concentration of the coating solution. Coated $LiCoO_2$ films were prepared using 0.05, 0.1, and 0.2 mol % coating solutions. The three coated samples obtained in this manner are hereafter called sample A (the sample fabricated using the 0.05 mol % coating solution), sample B (the sample fabricated using the 0.1 mol % coating solution), and sample C (the sample fabricated using the 0.2 mol % coating solution). Figure 1 presents scanning electron microscopy (SEM) images of the pristine and ZrO_2-coated $LiCoO_2$ thin films. In the cross sectional image, a columnar structure can be observed, with a thickness of about 4 μm. The surface of the film consisted of small polyhedral grains that were about 100-300 nm in size. The crystal faces and edges on the surface of the pristine $LiCoO_2$ film are very clear. As shown in Figure 2(b), no significant changes were observed in the surface image of sample A after it was coated with a thin coating layer. However, the morphology of the coated sample changed with an increase in the coating thickness. In the surface image of sample B (Fig. 1(c)), it seems that the valleys between the grains are sealed by the coating layer, even though the exact thickness of the coating layer cannot

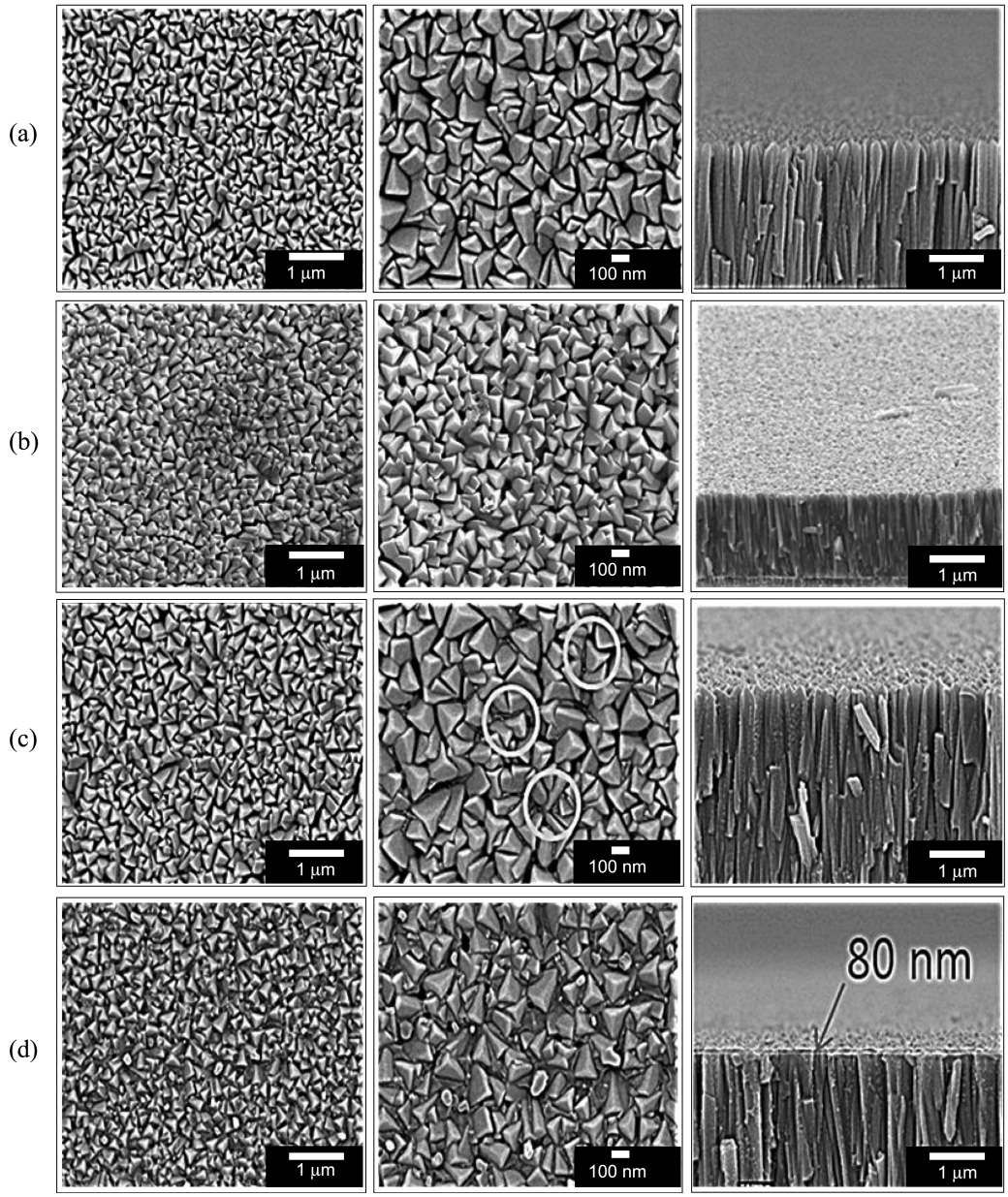

Figure 1. SEM images of pristine and ZrO_2-coated $LiCoO_2$ thin films (surface morphology is shown at left, and cross sectional image is shown at right): (a) pristine, (b) sample A, (c) sample B, and (d) sample C.

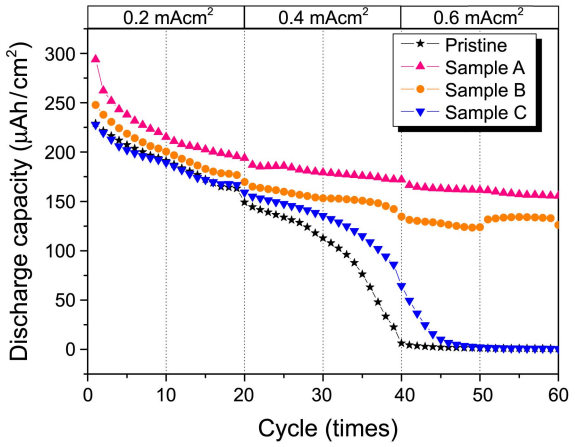

Figure 2. Discharge capacities and cyclic performances of pristine and coated $LiCoO_2$ thin films in voltage range of 4.25-3.0 V at current densities of 0.2, 0.4, and 0.6 mA·cm^{-2}.

be measured in the cross-sectional SEM image. Moreover, sample C shows a distinct coating layer in both the surface and cross sectional images. The thickness of the coating layer for sample C was measured to be about 80 nm. Based on the coating solution concentrations, it is estimated that the thicknesses of the sample coating layers had the following relationships: sample A < sample B < sample C.

In order to test the effects of the coating on the capacity, cyclic performance, and rate capability, the samples were cycled at various constant current densities. Figure 2 shows the discharge capacities and cyclic properties of the pristine and ZrO_2-coated $LiCoO_2$ thin films at current densities of 0.2, 0.4, and 0.6 mA·cm^{-2}, in the voltage range of 4.25-3.0 V. The current densities could be converted ~1 C, 2 C and 3 C rates, considering the average capacity of $LiCoO_2$ thin film is ~50 μAh/m^{-2}·μm. As shown in Figure 2, the coated samples showed slightly higher discharge capacities at all current densities compared to the pristine sample. It is interesting that the discharge capacity was improved by surface coating, because the ZrO_2 are non-active material of lithium ions, basically. However, considering high C rates in this measurement, the high capacities of the coated samples do not present improvement of theoretical capacity but imply enhancement of rate capability by surface coating. As expected, with an increase in the current density, the discharge capacity of the pristine film dropped rapidly. However, the coated samples showed greatly enhanced rate capabilities and cyclic performances. It is interesting that the electrochemical properties of the coated samples were highly dependent upon the coating thickness. Samples A and B,

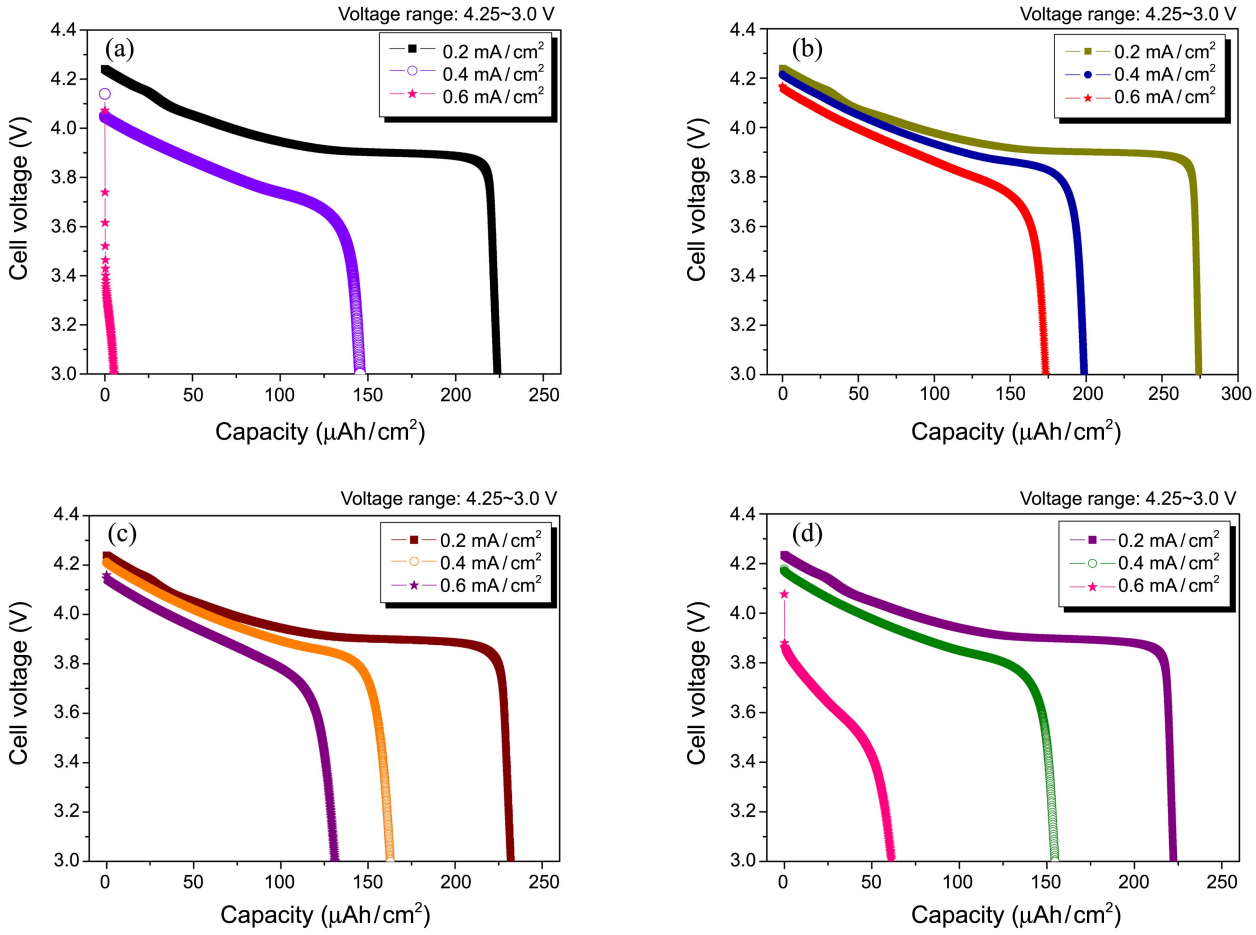

Figure 3. Initial discharge profiles of pristine and ZrO_2-coated $LiCoO_2$ thin film electrodes in voltage range of 4.25-3.0 V at current densities of 0.2 mA·cm^{-2}, 0.4 mA·cm^{-2}, and 0.6 mA·cm^{-2} (the first cycle of Fig. 2 at each current density): (a) pristine, (b) sample A, (c) sample B, and (d) sample C.

Table 1. Discharge capacities and capacity retention values of pristine and coated $LiCoO_2$ thin film samples at various C rates (values of initial cycle at respective C rates). (Percentages refer to capacity retention compared with discharge capacity at 0.2 C rate.)

	Pristine	(%)	Sample A	(%)	Sample B	(%)	Sample C	(%)
0.2 mA	229.07	100	293.84	100	247.83	100	227.66	100
0.4 mA	149.17	65.12	193.8	65.95	169.67	68.46	159.2	69.92
0.6 mA	6.27	2.37	171.85	58.48	134.58	54.30	64.47	28.32

which were considered to have thin coating layers, showed significantly enhanced discharge capacities at high current densities. In contrast, sample C, the $LiCoO_2$ film with the 80-nm thick ZrO_2 coating layer, displayed an inferior rate capability and cyclic performance compared to those of samples A and B, although its capacities at the current densities of 0.4 and 0.6 $mA{\cdot}cm^{-2}$ were slightly superior to those of the pristine film.

Figure 3 shows the voltage profiles of the pristine and coated samples at the current densities of 0.2, 0.4, and 0.6 $mA{\cdot}cm^{-2}$ as a function of the capacity (the first cycle of Fig. 2 at each current density). As seen, the rate capabilities of the coated samples were clearly improved. The discharge capacity of the pristine film at a current density of 0.6 $mA{\cdot}cm^{-2}$ was almost zero, whereas all of the coated films had improved capacity retention under the same measurement condition. In particular, the positive effect of the coating treatment on the rate capability was more prominent when the film had a thin coating layer. Sample A showed a capacity retention of ~58% at a current density of 0.6 $mA{\cdot}cm^{-2}$, compared with that at a current density of 0.2 $mA{\cdot}cm^{-2}$. Table 1 summarizes the discharge capacity and capacity retention values at the various current densities (the values of the initial cycles at the respective current densities). In this respect, it is clear that a ZrO_2 coating at a desirable thickness is effective at achieving a high rate capability. The enhancement of the rate capability by the surface coating is an interesting result, because the coating material conducts neither lithium ions nor electrons and so could obstruct their diffusion. However, this result could be explained by two types of theories. The first involves the protective effect of the coating layer. The surface of the cathode forms an interface layer during cycling because of the dissolution of the transition metals (Co, Ni, and Mn ions). This unwanted interface layer is a major obstacle to lithium and electron diffusion. The stable surface film layer can reduce the transition metal dissolution and suppress the formation of an unwanted surface layer, which leads to the enhanced rate capability of the coated cathode.[2,8] The other explanation involves the formation of a surface layer with high ionic conductivity because of the surface coating. The coating material could be diffused into the surface and react with the elements of the pristine electrode. Thus, the coating layer might not be able to maintain its original composition such as ZrO_2. In some cases, it is possible to form a kind of solid solution between the coating material and pristine cathode, which could act as a fast lithium ion conductor.[17] The improved electrochemical properties of Zr-doped $LiCoO_2$ powder have been reported.[20] However, if the coating thickness increased beyond the optimum value, the rate capability could have been deteriorated by the thick oxide layer interrupting lithium ion and electron movement.

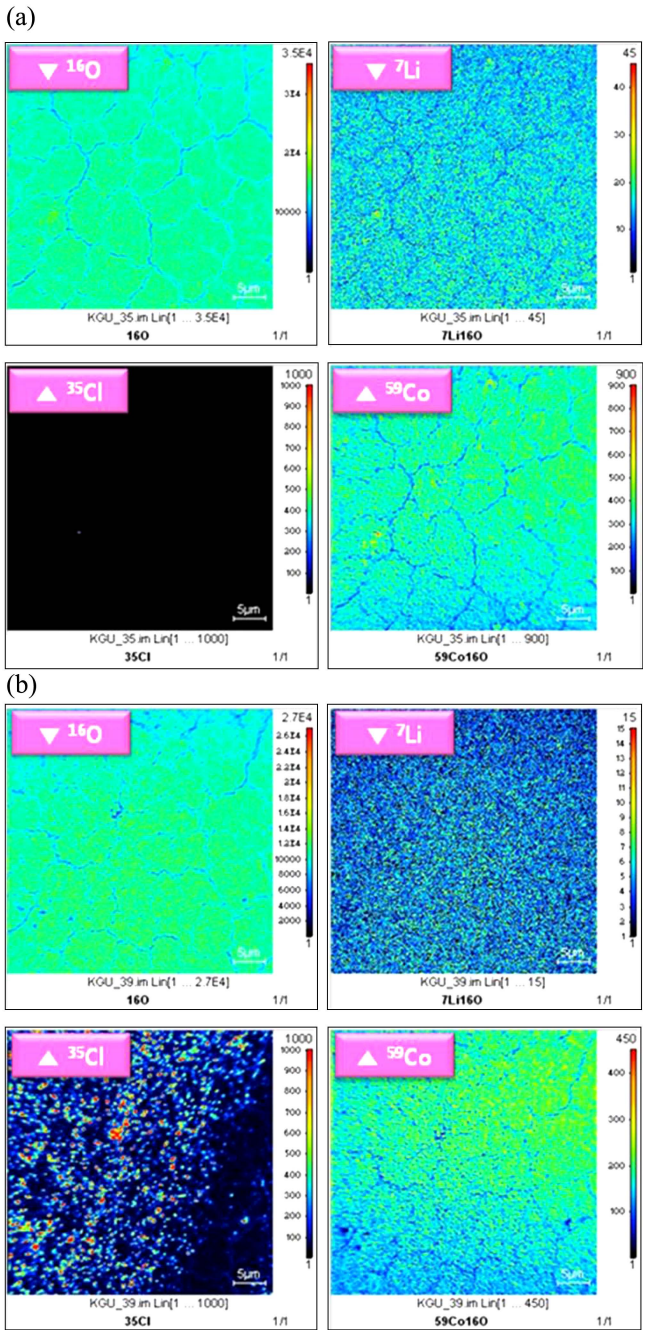

Figure 4. Constituent-element images of pristine $LiCoO_2$ thin film electrodes detected by SIMS analysis: (a) before cycling and (b) after cycling as shown in Fig. 2.

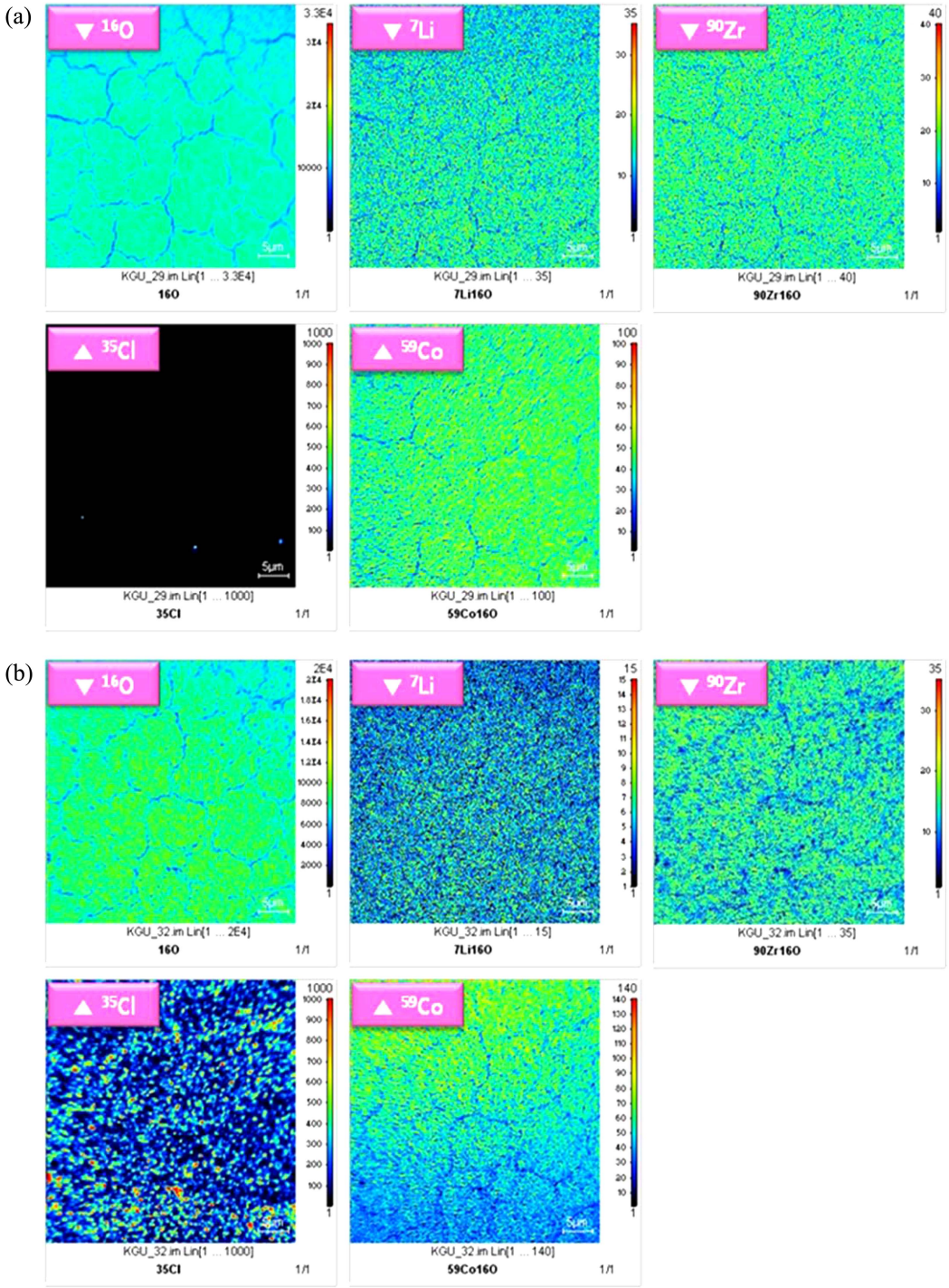

Figure 5. Constituent-element images of ZrO_2-coated $LiCoO_2$ thin film electrodes (sample B) detected by SIMS analysis: (a) before cycling and (b) after cycling as shown in Fig. 2.

After the cycling measurement in Figure 2, the constituent elements of the surface of the films were analyzed by secondary ion mass spectrometry (SIMS). Figure 4 shows the element images of the pristine sample obtained by the SIMS analysis. The spot intensity is an indicator of the element-concentration. In the image of the pristine sample before cycling (Fig. 4(a)), Li, Co, and O were detected uniformly on the surface. After cycling (Fig. 4(b)), the Li and Co concentrations seemed to have decreased because of the dissolution to the electrolyte, and Cl was detected because of the reaction with the electrolyte containing $LiClO_4$. Figure 5 presents the SIMS images of the surface of sample B (coated sample). In the image of Figure 5(a) (before cycling), Li, Co, O, and Zr were detected on the surface of the sample. In particular, the dense and uniform Zr spots in the images indicate that the ZrO_2 coating layer was successfully formed on the surface of the $LiCoO_2$ thin film. After cycling, the Li, Co, and Zr concentrations were

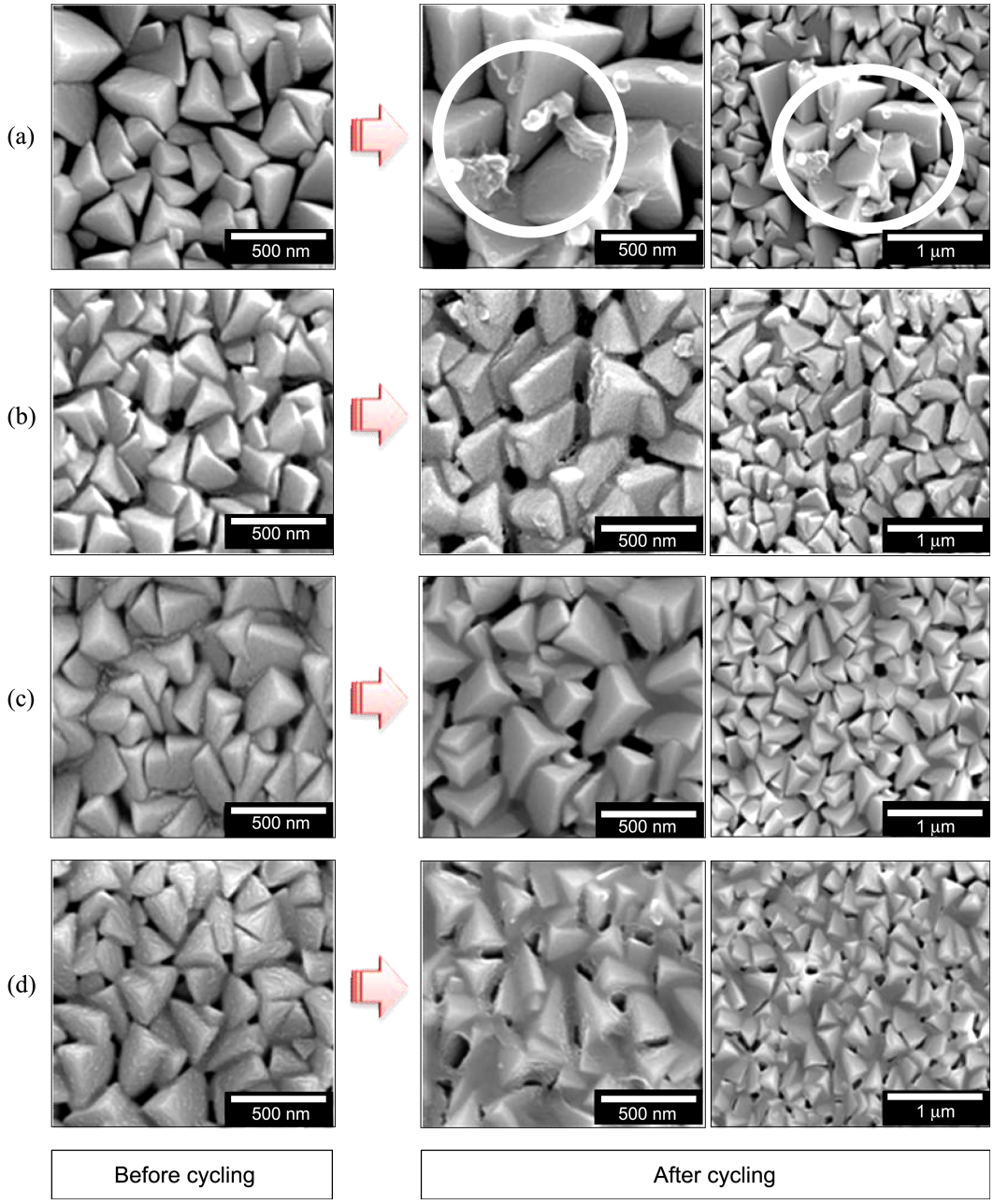

Figure 6. SEM images of pristine and ZrO_2-coated $LiCoO_2$ thin films before and after cycling: (a) pristine, (b) sample A, (c) sample B, and (d) sample C.

decreased, which was likely caused by a reaction with the electrolyte. The Zr coating layer seemed to be dissolved or damaged by the electrolyte, although the Zr coating layer was maintained during cycling. Cl was also detected on the surface of cycled sample B.

The surface morphological changes in the pristine and coated samples during cycling were investigated by SEM. As shown in Figure 6, noticeable morphology changes were observed in both the pristine and coated films. In the image of the pristine $LiCoO_2$ film (Fig. 6(a)), the original 100-300 nm grains are still observed, but larger grains (over 500 nm) can be seen on some parts of the surface (marked by a white circle on the right side of Fig. 6(a)). Furthermore, some small particles appear on the surface of the film. It is speculated that these small particles were formed from a reaction between the electrolyte and surface of the $LiCoO_2$ film. In contrast, these small particles were not detected on the surface of the coated samples. Instead, the coating layer could be distinguished more distinctly. The thickness of the coating layer seemed to be slightly increased, and the valleys between the grains were sealed more extensively by the coating layer after cycling, which was likely caused by a reaction with the electrolyte. However, the growth of the grains that was observed in the pristine film was not seen in the coated samples after cycling. The use of a film electrode will increase the surface reaction between a cathode and electrolyte because of its wide surface area. Thus, the damage to a cathode from an attack by an acidic electrolyte will

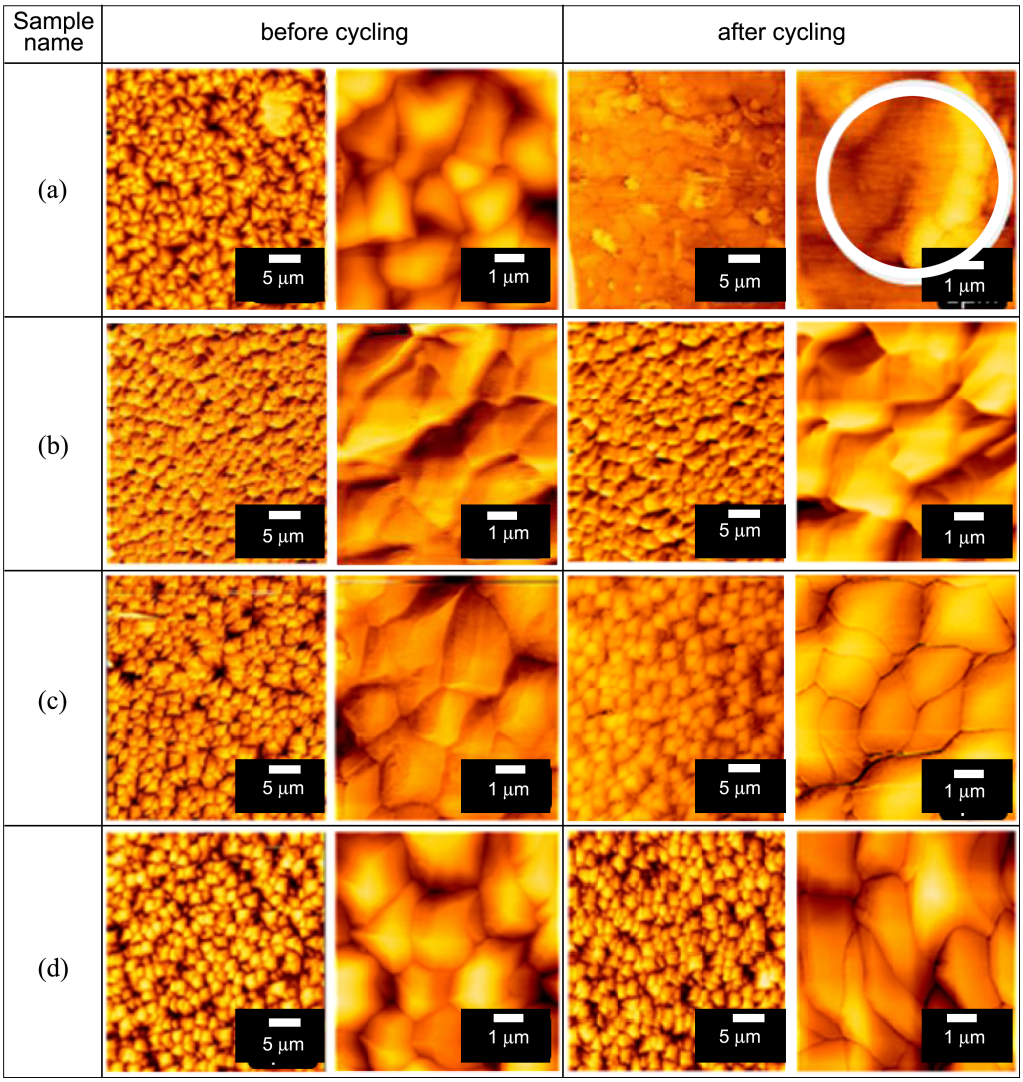

Figure 7. AFM images of pristine and ZrO_2-coated $LiCoO_2$ thin films before and after cycling: (a) pristine, (b) sample A, (c) sample B, and (d) sample C.

be observed more clearly. The growth of surface grains and the formation of small particles may show surface damage during cycling. The stable surface of the coated sample after cycling showed that the surface coating was effective at protecting the cathode from an unwanted reaction with the electrolyte. The growth of the coating layer after cycling seems to indicate that the coating layer itself reacted with the electrolyte instead of the cathode. However, the coating layer still acted as a protection layer after cycling, considering the electrochemical properties shown in Figures 2 and 3. The surface-morphological change in the pristine film was also confirmed by AFM analysis (Fig. 7). The surface of the pristine film before cycling was smooth and clean. However, after cycling the surface was clearly damaged and small particles (marked by a white circle in Fig. 7(a)) were also formed. However, the coated samples maintained smooth grains after cycling. This result clearly presents the protection effect of the ZrO_2 coating on the surface of the $LiCoO_2$ thin film.

Conclusions

We used a $LiCoO_2$ thin film electrode as a pristine cathode to investigate the interface reaction for an electrolyte/coating layer/pristine cathode in detail. A ZrO_2 film layer was successfully formed on the surface of the $LiCoO_2$ film using the sol-gel method with a spin coater. The ZrO_2 coating enhanced the discharge capacity and rate capability of the pristine $LiCoO_2$ film. However, these effects were highly dependent upon the coating thickness. SEM and AFM images showed that the surface of the pristine film was extensively damaged by a reaction with the electrolyte. However, this surface damage was dramatically suppressed by the ZrO_2 coating layer. The coated sample showed a very stable surface during cycling because of the protection effect of the coating layer.

Acknowledgments. This research was supported by the Basic Science Research Program through the National Re-

search Foundation of Korea (NRF) funded by the Ministry of Education, Science and Technology (2009-0071073).

References

1. Myung, S.-T.; Izumi, K.; Komaba, S.; Sun, Y.-K.; Yashiro, H.; Kumagai, N. *Chem. Mater.* **2005**, *17*, 3695.
2. Lee, H. J.; Park, K. S.; Park, Y. J. *J. Power Sources*. **2010**, *195*, 6122.
3. Amine, K.; Yasuda, H.; Yamachi, M. *Electrochem. Solid-State Lett.* **2000**, *3*, 178.
4. Thackeray, M. M.; Johnson, C. S.; Kim, J.-S.; Lauzze, K. C.; Vaughey, J. T.; Dietz, N.; Abraham, D.; Hackney, S. A.; Zeltner, W.; Anderson, M. A. *Electrochem. Commun.* **2003**, *5*, 752.
5. Myung, S.-T.; Izumi, K.; Komaba, S.; Yashiro, H.; Bang, H. J.; Sun, Y. K.; Kumagai, N. *J. Phys. Chem.* **2007**, *111*, 4061.
6. Lee, H.; Kim, Y.; Hong, Y. S.; Kim, Y.; Kim, M. G.; Shin, N.-S.; Cho, J. *J. Electrochem. Soc.* **2006**, *153*, A781.
7. Cho, J.; Kim, H.; Park, B. *J. Electrochem. Soc.* **2004**, *151*, A1707.
8. Ryu, K. S.; Lee, S. H.; Koo, B. K.; Lee, J. W.; Kim, K. M.; Park, Y. J. *J. Appl. Electrochem.* **2008**, *38*, 1385.
9. Cho, J.; Kim, Y. W.; Kim, B.; Lee, J. G.; Park, B. *Angew. Chem. Int. Ed*. **2003**, *42*, 1618.
10. Wu, Y.; Murugan, A. V.; Manthiram, A. *J. Electrochem. Soc.* **2008**, *155*, A635.
11. Zheng, J. M.; Zhang, Z. R.; Wu, X. B.; Dong, Z. X.; Zhu, Z.; Yang, Y. *J. Electrochem. Soc.* **2008**, *155*, A775.
12. Park, B.-C.; Kim, H.-B.; Myung, S.-T.; Amine, K.; Belharouak, I.; Lee, S.-M.; Sun, Y.-K. *J. Power Sources* **2008**, *178*, 826.
13. Yun, S. H.; Park, K. S.; Park, Y. J. *J. Power Sources* **2010**, *195*, 6108.
14. Yun, S. H.; Kim, S. B.; Park, Y. J. *Bull. Korean Chem. Soc.* **2009**, *30*, 2584.
15. Yun, S. H.; Park, Y. J. *Bull. Korean Chem. Soc.* **2010**, *31*, 355.
16. Hu, S. K.; Cheng, G. H.; Cheng, M. Y.; Hwang, B. J.; Santhanam, R. *J. Power Sources* **2009**, *188*, 564.
17. Kang, S. H.; Thackeray, M. M. *Electrochem. Commun.* **2009**, *11*, 748.
18. Liu, J.; Manthiram, A. *J. Electrochem. Soc*. **2009**, *156*, A66.
19. Liu, J.; Manthiram, A. *J. Electrochem. Soc*. **2009**, *156*, A833.
20. Xu, H. Y.; Xie, S.; Zhang, C. P.; Chen, C. H. *J. Power Sources* **2005**, *148*, 90.